

BEM stress analysis of 3D generally anisotropic elastic solids

C. L. Tan¹, Y.C. Shiah²

Summary

A BEM formulation for the numerical stress analysis of 3D generally anisotropic elastic solids is presented in this paper. It is based on closed-form algebraic expressions of the fundamental solutions derived by Ting and Lee [7] and Lee [8] which are defined in terms of Stroh's eigenvalues, and has never been implemented previously in the literature. The veracity of the formulation and implementation is demonstrated by two engineering examples.

Introduction

The boundary element method (BEM) is well recognized as a very efficient numerical tool for the elastic stress analysis of solids, particularly those with high stress gradients. Although well established for isotropic elastostatics, and for 2D anisotropic elasticity, its development for 3D anisotropic elasticity in the past three decades has been sporadic and less mature. This is because of the mathematical complexity of the fundamental solutions which are necessary items in the formulation of the boundary integral equation (BIE), and the computational burden to evaluate them. In the pioneering work of Wilson and Cruse [1], the Green's function for displacements employed and its derivatives, which are in terms of a contour integral over a unit circle, are evaluated numerically into a database, from which interpolation of the stored values is carried out in the BEM calculations. It is, however, demanding on computer storage requirements and in addition, may not provide sufficient accuracy for materials with high degree of anisotropy. Sales et al. [2] and Phan et al. [3] had proposed more efficient schemes to evaluate the 3D fundamental solutions, but there was no report of their implementation into a BEM formulation. Other BEM implementations that have been developed include that by Tonon et al.[4], and more recently, by Wang and Denda [5]. Both are based on a more explicit Green's function solution [6] in which the algorithm to compute it involves contour integration over a rectangular parallelepiped, and over a semi-circle, respectively.

An alternative, explicit, real-variable, algebraic form of the fundamental solutions for the displacements and its derivatives for 3D generally anisotropic solids have been derived by Ting and Lee [7] and Lee [8], respectively. They are expressed in terms of Stroh's eigenvalues and can be evaluated in fairly straight-forward manner involving primarily multiplication of matrices related to the material properties

¹Dept. of Mechanical & Aerospace Engineering, Carleton University, Ottawa, Canada K1S 5B6

²Dept. of Aerospace and Systems Engineering, FengChia University, Taichung, Taiwan R.O.C.

and the field point position. Their veracity has been demonstrated recently [9]; surprisingly, they have never been employed previously in BEM. In this paper, these fundamental solutions are used in a conventional BEM formulation for 3D generally anisotropic elastostatics. The implementation has been successfully carried out by modifying a code which had been previously developed for 3D isotropic elasticity using quadratic isoparametric elements [10]. As this numerical algorithm is well-established in the literature, only the explicit-form fundamental solutions employed are presented next. The success of the implementation is then illustrated by two examples involving stress concentrations in engineering stress analysis.

Fundamental Solutions

Only the final forms of the fundamental solutions are presented here, the reader is referred to [7] and [8] for more details of their derivation. Consider a source point P in an infinite anisotropic body at the local origin $\mathbf{x} = \mathbf{0}$ where a unit load is applied, and the field point Q at $\mathbf{x} = (x_1, x_2, x_3)$ at distance r away. For a unit circle $|\mathbf{n}^*|$ on an oblique plane normal to \mathbf{x}_Q , the unit vector \mathbf{n}^* can be written in terms of an arbitrary parameter ψ as

$$\mathbf{n}^* = \mathbf{n} \cos \psi + \mathbf{m} \sin \psi, \quad (1)$$

where the vectors \mathbf{n} , \mathbf{m} along with \mathbf{x}/r form a right-handed triad $[\mathbf{n}, \mathbf{m}, \mathbf{x}/r]$. By introducing the following three tensors,

$$Q \equiv Q_{ik} = C_{ijks} n_j n_s, \quad R \equiv R_{ik} = C_{ijks} n_j m_s, \quad T \equiv T_{ik} = C_{ijks} m_j m_s, \quad (2)$$

where C_{ijks} is the material stiffness matrix, Ting and Lee [7] have obtained the Green's function for displacements, $\mathbf{U}(\mathbf{x})$, to be

$$\mathbf{U}(\mathbf{x}) = \frac{1}{4\pi r} H_{ij} = \frac{1}{4\pi r} \frac{1}{|\mathbf{T}|} \sum_{n=0}^4 q_n \bar{\Gamma}^{(n)}, \quad (3)$$

where $\bar{\Gamma}$, with components $\bar{\Gamma}^{(n)}$, is the adjoint of Γ and

$$\Gamma(p) = \mathbf{Q} + p(\mathbf{R} + \mathbf{R}^T) + p^2 \mathbf{T}. \quad (4)$$

In eq.(8), $p = \tan \psi$ and a sextic equation in p is obtained by setting the determinant, $|\Gamma(p)|$, to zero. The six independent roots of this equation are complex, $p_v = \alpha_v + i\beta_v$, $\beta_v > 0$, ($v = 1, 2, 3$), and they appear as conjugate pairs; they are the Stroh's eigenvalues. Also in eq. (3), q_n is given by

$$q_n = \begin{cases} \frac{-1}{2\beta_1\beta_2\beta_3} \left[\mathbf{Re} \left\{ \sum_{t=1}^3 \frac{p_t^n}{(p_t - \bar{p}_{t+1})(p_t - \bar{p}_{t+2})} \right\} - \delta_{n2} \right] & \text{for } n = 0, 1, 2, \\ \frac{-1}{2\beta_1\beta_2\beta_3} \left[\mathbf{Re} \left\{ \sum_{t=1}^3 \frac{p_t^{n-2} \bar{p}_{t+1} \bar{p}_{t+2}}{(p_t - \bar{p}_{t+1})(p_t - \bar{p}_{t+2})} \right\} \right] & \text{for } n = 3, 4, \end{cases} \quad (5)$$

where the overbar in p_t denotes the complex conjugate, δ_{ij} is the Kronecker delta and the subscript t follows the cyclic rule $t = (t - 3)$ if $t > 3$. More explicit expressions of $\bar{\mathbf{\Gamma}}^{(n)}$ in terms of \mathbf{Q} , \mathbf{R} and \mathbf{T} may be found in [9].

The traction fundamental solution, $\mathbf{T}^*(\mathbf{x})$, is obtained via the first derivative of the Green's function for displacements, and invoking the generalized Hooke's law and the well-known relationship between the stress tensor and traction vector. Thus, only the displacement derivative of $\mathbf{U}(\mathbf{x})$ as derived by Lee [8] is presented here, as follows:

$$U_{ij,l} = \frac{1}{4\pi^2 r^2} \left[-\pi y_l H_{ij} + C_{pqrs} (y_s M_{lqiprj} + y_q M_{stiprj}) \right] \quad (6)$$

where

$$M_{ijklmn} = \frac{2\pi i}{|T|^2} \sum_{t=1}^3 \frac{1}{(p_t - p_{t+1})^2 (p_t - p_{t+2})^2} \left[\Phi'_{ijklmn}(p_t) - 2\Phi_{ijklmn}(p_t) \times \left(\frac{1}{p_t - p_{t+1}} + \frac{1}{p_t - p_{t+2}} \right) \right] \quad (7)$$

$$\Phi_{ijklmn}(p) = \frac{[n_i n_j + (n_i m_j + m_i n_j) p + m_i m_j p^2] [\hat{\Gamma}_{kl}(p) \hat{\Gamma}_{mn}(p)]}{(p - \bar{p}_1)^2 (p - \bar{p}_2)^2 (p - \bar{p}_3)^2} \quad (8)$$

In eq. (11), the prime in $\Phi'_{ijklmn}(p_t)$ denotes differentiation with respect to p . It is not necessary to rewrite this term as a fully explicit expression, since it is a relatively simple matter to program the functions $\hat{\Gamma}(p)$, $(p - \bar{p}_t)^2$, $[n_i n_j + (n_i m_j + m_i n_j) p + m_i m_j p^2]$, and their derivatives into subroutines in the computer code and then apply the chain rule in the differentiation.

Numerical Results

Due to space limitations, only two examples are presented here to demonstrate the veracity and capability of the BEM formulation developed. Both problems had been solved first in isotropy using the 3D BEM isotropic algorithm, and then re-solved using the present algorithm for 3D anisotropic elasticity as a check; nearly identical results were obtained. For the two example problems, the following anisotropic stiffness coefficients corresponding to alumina were employed:

$$\mathbf{C} = \begin{bmatrix} 465 & 124 & 117 & 101 & 0 & 0 \\ 124 & 465 & 117 & -101 & 0 & 0 \\ 117 & 117 & 563 & 0 & 0 & 0 \\ 101 & -101 & 0 & 233 & 0 & 0 \\ 0 & 0 & 0 & 0 & 233 & 101 \\ 0 & 0 & 0 & 0 & 101 & 170.5 \end{bmatrix} \text{ GPa}$$

The first example, shown in Fig.1, is a rectangular plate with a central hole subject to remote uniaxial tension, σ_o , in the x_3 -direction at the top face and restrained at the bottom face. Table 1 lists the stress concentration factor, $k = \sigma_{33}/\sigma_o$, at the edge of the hole for this geometry in the mid-thickness plane (where it is largest) as obtained from the present 3D anisotropic analysis. Also shown for comparison are the corresponding results from an ANSYS FEM anisotropic and BEM isotropic analysis (with Poisson's ratio $\nu = 0.3$).

Table 1: BEM computed stress concentration factor, $k = \sigma_{33}/\sigma_o$ - Example 1

3D Anisotropy (BEM)	3D Anisotropy (ANSYS)	3D Isotropy (BEM)
3.2778	3.227	3.197

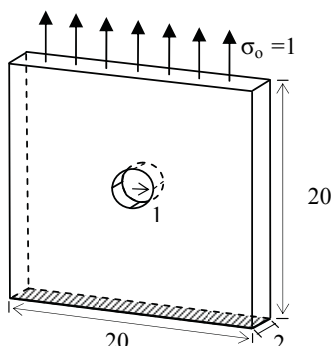


Figure 1: Example 1

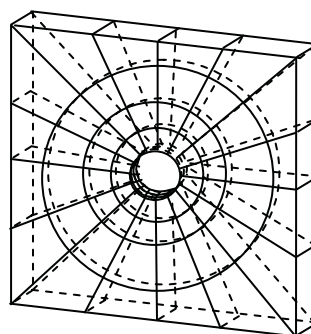


Figure 2: BEM mesh: Ex. 1

The second example considered is a cylindrical bar with a spherical cavity under remote tension, σ_o , as shown in Fig. 3. A range of relative cavity sizes were considered, with $a/R = 0.2$ to 0.5 , where a and R are the radii of the cavity and bar, respectively. A typical BEM 3D mesh employed is shown in Fig. 4. Figure 5 shows the variation of the stress concentration $k = \sigma_{33}/\sigma_o$ with the relative size of the cavity as measured by a/R ; the corresponding results obtained from ANSYS FEM anisotropic analysis and from the BEM isotropic analysis are also shown for comparison.

It can be seen that agreement between the 3D BEM and FEM results for both examples is very good indeed. The deviations of k from the corresponding isotropic cases are also very small; this is not too surprising in view of the near quasi-isotropy in the $x_1 - x_2$ plane and not very severe anisotropy in the $x_1 - x_3$ plane.

References

1. Wilson, R.B.; Cruse, T.A. (1978): Efficient implementation of anisotropic three dimensional boundary integral equation stress analysis. *Int. J. Numer.*

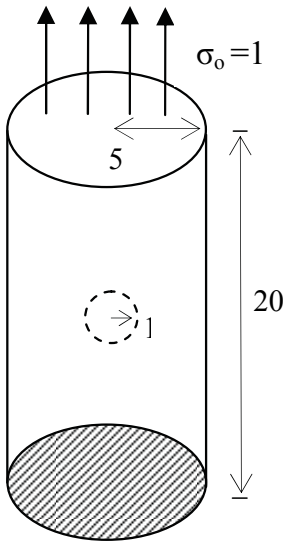


Figure 3: Example 2

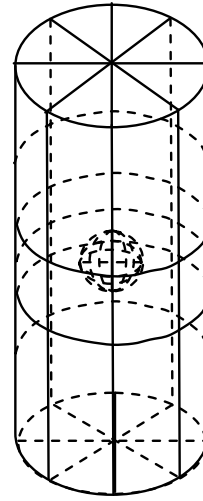


Figure 4: Typical BEM mesh: Ex. 2

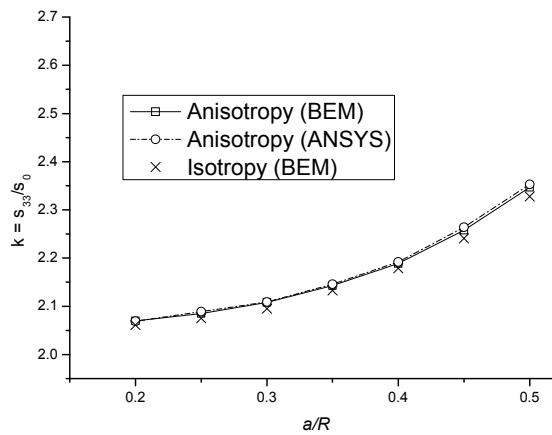


Figure 5: Variation of stress concentration factor, $k = \sigma_{33}/\sigma_0$, with a/R – Example 2.

Methods Engng., 12, 1383-1397.

2. Sales, M.A.; Gray, L.J. (1998): Evaluation of the anisotropic Green's function and its derivatives. *Comp. & Struct.*, 69, 247-254.
3. Phan, P.V.; Gray, L.J.; Kaplan, T. (2004): On the residue calculus evaluation of the 3D anisotropic elastic Green's function. *Comm. Numer. Methods Engng.*, 20, 335-341.
4. Tonon, F.; Pan, E.; Amadei, B. (2001): Green's functions and boundary el-

- ement method formulation for 3D anisotropic media. *Comp. & Struct.*, 79, 469-482.
5. Wang, C.Y.; Denda, M. (2007): 3D BEM for general anisotropic elasticity. *Int. J. Solids Struct.*, 44, 7073-7091.
 6. Wang, C.Y. (1997): Elastic fields produced by a point source in solids of general anisotropy. *J. Engng. Math.*, 32, 41-52.
 7. Ting, T.C.T.; Lee, V.G. (1997): The 3D elastostatic Green's function for general anisotropic linear elastic solid. *Q. J. Mech. Appl. Math.*, 50, 407-426.
 8. Lee, V.G. (2003): Explicit expression of derivatives of elastic Green's functions for general anisotropic materials. *Mech. Res. Comm.*, 30, 241-249.
 9. Shiah, Y.C.; Tan, C.L.; Lee, V.G.; Chen, Y.H. (2008): Evaluation of Green's functions for 3D anisotropic elastic solids. *Advances in Boundary Element Techniques IX, Proc. BeTeq 2008 Conf., Seville*, R. Abascal & M.H. Aliabadi (eds.), E.C. Ltd. (U.K.), pp. 119-124.
 10. Tan, C.L.; Fenner, R.T. (1979): Elastic fracture mechanics analysis by the boundary integral equation method. *Proc. Royal Soc. London*, A369, 243-260.